Characterization of the Ni–Fe–C Complex Formed by Reaction of Carbon Monoxide with the Carbon Monoxide Dehydrogenase from *Clostridium thermoaceticum* by Q-Band ENDOR†

Chaoliang Fan,‡ Carol M. Gorst,§ Stephen W. Ragsdale,*,§ and Brian M. Hoffman*,‡

Department of Chemistry, Northwestern University, Evanston, Illinois 60208, and Department of Chemistry, University of Wisconsin—Milwaukee, Milwaukee, Wisconsin 53201

Received June 22, 1990; Revised Manuscript Received August 8, 1990

ABSTRACT: Q-Band ENDOR studies on carbon monoxide dehydrogenase (CODH) from the acetogenic bacterium *Clostridium thermoaceticum* provided unambiguous evidence that the reaction of CO with CODH produces a novel metal center that includes at least one nickel, at least three iron sites, and the carbon of one CO. The ^{57}Fe hyperfine couplings determined by ENDOR are similar to the values used in simulation of the Mössbauer spectra [Lindahl et al. (1989) *J. Biol. Chem. 265*, 3880–3888]. EPR simulation using these A^{Fe} values is equally good for a 4Fe or a 3Fe center. The ^{13}C ENDOR data are consistent with the binding of a carbon atom to either the Ni or the Fe component of the spin-coupled cluster. The ^{13}C hyperfine couplings are similar to those determined earlier for the CO-bound form of the H cluster of the *Clostridium pasteurianum* hydrogenase, proposed to be the active site of hydrogen activation [Telser et al. (1987) *J. Biol. Chem. 262*, 6589–5694]. The ^{61} Ni ENDOR data are the first nickel ENDOR recorded for an enzyme. The EPR simulation using the ENDOR-derived hyperfine values for ^{61}Ni is consistent with a single nickel site in the Ni–Fe–C complex. On the basis of our results and the Mössbauer data [Lindahl et al. (1989) *J. Biol. Chem.* 265, 3880–3888], we propose the stoichiometry of the components of the Ni–Fe–C complex to be $Ni_1Fe_{3-4}S_{\geq 4}C_1$, with four acid-labile sulfides.

Carbon monoxide dehydrogenase (CODH) fromthe acetogenic bacterium *Clostridium thermoaceticum* (Ragsdale & Wood, 1985) catalyzes the oxidation of CO to CO_2 (eq 1) and the synthesis of acetyl-CoA from a methylated corrinoid protein ([Co]protein), CO, and CoA (eq 2). The enzyme has

$$CO + H_2O \rightleftharpoons CO_2 + 2H^+ + 2e^- \quad (1)$$

$$CH_3[Co]protein + CO + CoASH \rightarrow CH_3C(O)SCoA + [Co]protein \quad (2)$$

an $(\alpha\beta)_3$ hexameric structure, and each $\alpha\beta$ dimer contains 1 Zn, 2 Ni, 11–13 Fe, and 14 inorganic S (Ragsdale et al., (1983a). The metals are arranged into a variety of complexes with poorly understood structures.

The oxidized enzyme is EPR-silent. Reduction of the enzyme in the absence of CO yields EPR signals that are quite complicated and difficult to interpret. A signal from a 4Fe cluster first appears at g = 2.01, 1.81, and 1.65 (g_{av} = 1.82) with a midpoint potential of −215 ± 35 mV. Upon further reduction, there appear two overlapping signals with the same g values, g = 2.04, 1.94, and 1.90 (g_{av} = 1.94), but different line widths; these are assigned to two conformations of a $[4Fe\text{–}4S]^{2+/1+}$ cluster (Lindahl et al., 1984, 1989b). An EPR signal with g = 1.94, 1.87, and 1.75 (g_{av} = 1.86) and a midpoint potential of −530 ± 30 mV is observed in the fully reduced enzyme. The g_{av} = 1.82 species converts into the g_{av} = 1.86 species as the redox potential is lowered (Lindahl et al., 1989b).

Treatment of oxidized CODH with CO reduces the enzyme and elicits EPR signals due to the reduced Fe–S clusters mentioned above (Ragsdale et al., 1982). In addition, there appears a new EPR signal with g values of 2.074 and 2.028. On the basis of the finding that this signal exhibits hyperfine broadening upon ^{61}Ni, ^{57}Fe, and ^{13}C isotopic enrichment, it has been called the Ni–Fe–C signal and has been assigned to a unique enzyme-bound complex that contains nickel, iron, and a carbon from CO (Lindahl et al., 1989b; Ragsdale et al., 1983b, 1985). The CO of this mixed-metal carbonyl species (CODH–CO) acts as an intermediate in the synthesis of acetyl-CoA. We also observe variable amounts of a signal with g values (2.067, 2.054, and 2.028) that appears to be due to an altered conformation of the (2.074, 2.028) species (Ragsdale et al., 1985). The relative amounts of the two signals are affected by the presence of the substrates, CoA and acetyl-CoA (Ragsdale et al., 1985), and complete conversion of the (2.067, 2.054, 2.028) signal into the (2.074, 2.028) signal can be effected by treatment of CODH with *N*-bromosuccinamide, which modifies tryptophan residues near the CoA binding site (Shanmugasundaram et al., 1988). When the CODH from methanogenic bacteria is incubated with CO, EPR signals similar to those from the Ni–Fe–C species from *C. thermoaceticum* have been observed (Terlesky et al., 1987). Interconversion between two forms of the CODH–CO complex from methanogen also can be observed by treatment with CO in the presence of CoA and acetyl-CoA (Terlesky et al., 1987). The EPR signature of the Ni–Fe–C species appears to be lacking in the nickel-containing CODH from *Rhodospirillum rubrum*; however, the *R. rubrum* protein contains a Ni–Fe–S center with g values at 2.04, 1.90, and 1.71 (Stephens et al., 1989). This EPR signal is similar in appearance to the g_{av} = 1.82 EPR signal described above for the CODH from *C. thermoaceticum*.

Identification of the structure of this Ni–Fe–C center of CODH is important because it appears to be the binding site for CO and CO_2 in the synthesis of acetyl-CoA, in the oxidation of CO to CO_2, and in the reduction of CO_2 to CO.

† This work has been supported by the NSF (DBM-8606575, B.M.H.), the NIH (HL 13531, B.M.H.), the DOE (FGO2-88ER13875, S.W.R), and The Shaw Scholars Award (S.W.R.).

‡ Northwestern University.

§ University of Wisconsin—Milwaukee.

0006-2960/91/0430-431$02.50/0

Reduction of CO_2 to CO occurs at redox potentials near the thermodynamic equilibrium potential (Lindahl et al., 1989b), which is important for chemists seeking to find efficient catalysts for CO-dependent reactions. Recent evidence also indicates that this Ni–Fe center could be the site of assembly of the acetyl–CODH complex (site of formation of CH_3–C-ODH, CODH–CO, and acetyl–CODH), which is the direct precursor of the acetyl group of acetyl-CoA (Lu & Ragsdale, 1990). Besides the EPR studies described above, Mössbauer (Lindahl et al., 1989a) and X-ray absorption (XAS) studies have been performed in order to determine the structure of the CODH–CO intermediate (Cramer et al., 1987; Bastian et al., 1988). XAS studies indicate a sulfur-rich Ni environment (Cramer et al., 1987; Bastian et al., 1988) and a Ni–Fe distance consistent with a Ni–X–Fe bridge (Bastian et al., 1988).

Electron–nuclear double-resonance (ENDOR) techniques provide an ideal tool to characterize the metal sites of CODH (Hoffman et al., 1990). In the experiments reported here, this Ni–Fe–C complex is unambiguously identified using Q-band (35 GHz) ENDOR spectroscopy.

Materials and Methods

C. thermoaceticum was grown on glucose at 55 °C as described (Ljungdahl & Andreesen, 1978). For the ^{57}Fe experiments, $^{57}Fe_2O_3$ (Oak Ridge National Laboratories) was dissolved in HCl and added to the medium to a final concentration of 26 μM, giving an approximate isotope purity of 85%. For the ^{61}Ni experiments, ^{61}Ni (88.8% isotopic purity) was dissolved in concentrated nitric acid and added to 7 μM final concentration in the growth medium, giving a calculated isotope purity of 86%. For the ^{13}C experiments, nonisotopically labeled CODH was treated with ^{13}CO (99% isotopic purity, Merck and Co.). The Ni–Fe–C species was generated in each case by reacting the enzyme with CO for 5–10 min before freezing in liquid nitrogen. The specific activities of the different enzyme preparations in the CO oxidation reaction (Ragsdale et al., 1983a) and the CO/acetyl-CoA exchange reaction (Ragsdale et al., 1985) were 80 units/mg and 30 milliunits/mg for the ^{13}CO enzyme preparation, 200–300 units/mg and 500 milliunits/mg for the ^{57}Fe CODH, and 500 units/mg in the CO oxidation reaction for the ^{61}Ni CODH.

X-Band EPR spectroscopy of CODH after reaction with CO as described was performed on a Varian Model E-115 spectrometer with a digital frequency meter (Model 548A, EIP Microwave Inc., San Jose, CA). Temperature was maintained at 100 K with a variable-temperature controller (Varian). Simulations of the spectra were performed with the program XPOW (Altman, 1981; Belford & Nilges, 1979; Duliba, 1981; Maurice, 1981; Nilges, 1981) which was obtained from the Illinois ESR Center, NIH Grant RR01811. The simulations included the percentage isotopic enrichment, calculated from the initial enrichment and the known amount of natural-abundance isotope initially in the medium (above). In addition, variable amounts of the two forms of the Ni–Fe–C signal were given identical hyperfine splitting values. The g values used in the simulations had been determined earlier (Ragsdale et al., 1985), and the A values were obtained from the ENDOR data. For futher, details, see the figure legend to Figure 4.

ENDOR absorption spectra were recorded on a modified Varian 35-GHz (Q-band) spectrometer. The instrumentation is similar to the 9.5-GHz (X-band) ENDOR spectrometer (Venters et al., 1986), except that a Varian E110 microwave bridge is interfaced to the E190 EPR console. Experiments were performed with a silvered TE_{011} sample cavity held at about 2 K in a Janis Corp. liquid helium immersion dewar; mutually perpendicular field-modulation and radio-frequency coils run through the cavity.

ENDOR is performed at a fixed applied field, H_0, and is manifested by changes in the EPR signal intensity that result from nuclear transitions induced by a swept radio-frequency field (Feher, 1959). The ENDOR transition frequency of a nucleus, J, with $I = {}^1/_2$ is given by the equation

$$\nu_\pm = |\nu_J \pm A^J/2| \qquad (3)$$

The ENDOR spectrum of the protons at Q-band, normally $\nu_H > A^H/2$, shows a pair of lines separated by the angle-dependent hyperfine coupling constants, A^H, and mirrored about the free-proton Larmor frequency $\nu_H = g_H\beta_n H_0/h$ (42.6 MHz at 10 kG), whereas the ENDOR spectrum of ^{57}Fe, normally $A^{Fe}/2 > \nu_{Fe}$, appears as a pair of lines centered at $A^{Fe}/2$ and split by $2\nu_{Fe}$. A nucleus, K, having $I \geq 1$, such as ^{14}N (I = 1) or ^{61}Ni ($I = {}^3/_2$), can exhibit an angle-dependent quadrupole interaction term, P^K, as well as the nuclear Zeeman and hyperfine term, and its possible ENDOR frequencies are (Hoffman et al., 1990)

$$\nu_\pm(m) = |\pm A^K/2 + \nu_K + (2m - 1)3P^K/2| \qquad (4)$$

where $-I^K + 1 \leq m \leq I^K$. The result is a pattern centered at the frequency $A^K/2$ or ν_K, whichever is larger, and having as many as $4I^K$ lines. The splitting by the quadrupole interaction has not been resolved in the ^{61}Ni ENDOR measurements we report in this paper. Although the signs of the hyperfine couplings in a spin-coupled system are significant, they are not given by these ENDOR experiments, and couplings are given as positive values.

Q-Band (35 GHz) ENDOR has an additional key advantage over X-band. At X-band (9.5 GHz), the ENDOR signals of ^{14}N, ^{57}Fe, etc. commonly fall within the more intense proton ENDOR pattern ($\nu_H \approx 14$ MHz) and thus are difficult, often impossible, to detect. At Q-band, however, the proton ENDOR pattern shifts to a center-frequency of $\nu_H \approx 50$ MHz, whereas the ^{14}N, ^{57}Fe, etc. resonances remain, unobscured, in the range $\nu < 30$ MHz.

Results and Discussion

The 2 K EPR spectrum of the reduced *C. thermoaceticum* CODH at Q-band frequency exhibits athe Ni–Fe–C signal ($g_\perp$ = 2.08 and $g_\parallel$ = 2.03) as well as the signals from 4Fe clusters with g_{av} = 1.94 and with g_{av} = 1.82. The Ni–Fe–C signal overlaps with the signals from 4Fe cluster at field positions where $2.03 \lesssim g \lesssim 2.04$. Thus, within this field range, ENDOR signals would arise from both types of center.

^{57}Fe ENDOR. ^{57}Fe ENDOR signals from the ^{57}Fe-enriched enzyme are readily observed at various field positions across the EPR signals from the Ni–Fe–C center and the Fe–S clusters.

When the magnetic field is set of $H_0 < 12230$ G ($g > 2.06$), where the Ni–Fe–C signal dominates, three ENDOR lines are observed at 11.9, 15.8, and 19.1 MHz (Figure 1A); these ENDOR signals are absent in a ^{56}Fe sample and not detected from reduced ^{57}Fe-enriched sample without the Ni–Fe–C signal and thus are assigned as ^{57}Fe resonances associated with the Ni–Fe–C center. This signal at 11.9 MHz is better resolved if the radio-frequency field is scanned from low to high frequency, while the one at 19.1 MHz is better resolved if the scan is in the opposite direction.

A simple interpretation of these ^{57}Fe signals from the Ni–Fe–C center is that they are associated with a single type of iron site, representing one or more equivalent iron ions. The peaks at 15.8 and 19.1 MHz are split by $2\nu_{Fe}$ = 3.3 MHz and thus represent a ^{57}Fe Larmor split doublet centered at $A^{Fe}/2$

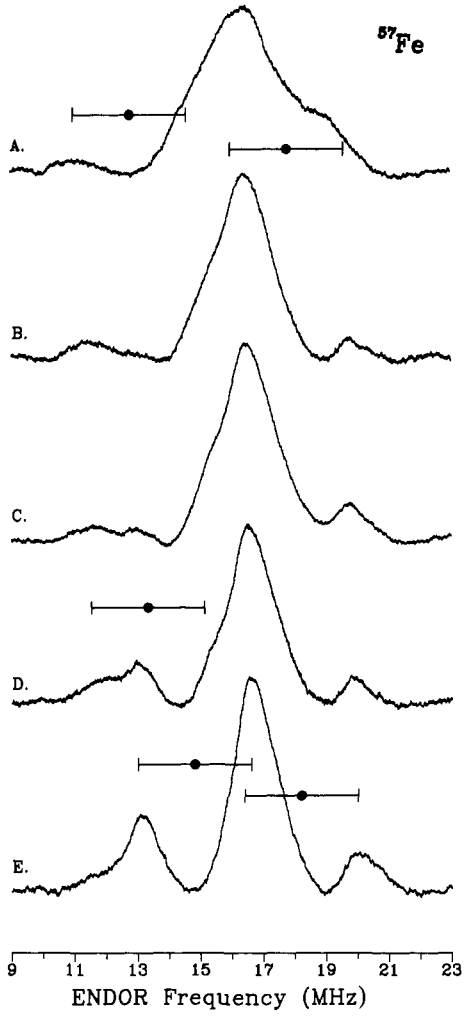

FIGURE 1: ^{57}Fe ENDOR spectra for ^{57}Fe-enriched *C. thermoaceticum* CODH. The symbol (|-●-|) indicates the frequency corresponding to $A^{Fe}/2$ (●) and the Larmor splitting of $2\nu_{Fe}$ (|—|). Analogous markers are presented in the other figures. *Conditions*: T = 2 K; microwave power, ~35 mW; microwave frequency, 35.22 GHz; H = 12070 (A), 12230 (B), 12250 (C), 12270 (D), and 12300 G (E); 100-kHz field modulation, 2.5 G; rf scan rate, 1.5 MHz/s; scans, ~400.

= 17.4 MHz. The weak feature at 11.9 MHz could arise from the anisotropy of the iron hyperfine coupling; an ENDOR simulation, using $A_\perp$ = 35 and $A_\parallel$ = 27 MHz with the hyperfine tensor rotated by 45° about the g_2 axis of the g tensor, fits the spectra taken around $g_\perp$ quite well. An alternative interpretation is that ENDOR signal arises from two similar but inequivalent iron sites, with $A^{Fe}(1)$ = 27 and $A^{Fe}(2)$ = 35 MHz as indicated in Figure 1A; in this case, the signal at 15.8 MHz would represent the superposition of the ν_+ feature of site 1 and the ν_- transition of site 2.

The ENDOR measurement cannot quantitate the number of equivalent nuclei associated with a ^{57}Fe doublet. However, comparison of the ENDOR results, which require the ^{57}Fe hyperfine couplings to be less than 35 MHz, with those of EPR line broadening (Ragsdale et al., 1988), which gave $A_\parallel$ = 40 and $A_\perp$ = 60 MHz if the Ni–Fe–C center contains one iron ion or $A_\parallel$ = 20 and $A_\perp$ = 30 MHz if it contains two, requires that the Ni–Fe–C cluster contains more than a single iron ion. Simulation (Figure 4) of the line broadening of the X-band EPR spectrum upon ^{57}Fe substitution, using the A^{Fe} obtained by ENDOR measurements, suggests that either three or four irons are involved in formation of this Ni–Fe–C center. The simulation using four iron gives a slightly better fit. The

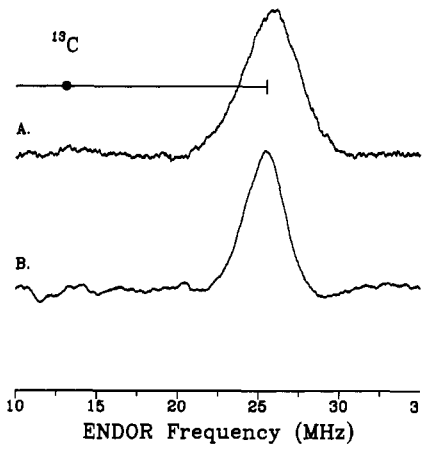

FIGURE 2: ^{13}C ENDOR spectrum from CODH treated with ^{13}CO. *Conditions*: microwave frequency, 35.22 GHz; H = 12000 (A) and 12400 G (B); rf scan rate, 5.0 MHz/s; scans, 500. Other conditions are the same as Figure 1.

possibility of four iron is also supported by Mössbauer spectroscopy of the ^{57}Fe labeled enzyme (discussed below).

We have shown in ^{57}Fe ENDOR studies of other systems that examination of the field dependence of the ^{57}Fe signals from the Ni–Fe–C center would allow a complete analysis that fully describes the iron sites of the Ni–Fe–C center. Unfortunately, a large portion of the EPR spectrum of this center overlaps with that of the [4Fe–4S] cluster with g_{max} at 2.04, so that the ^{57}Fe ENDOR signals from the Ni–Fe–C and this [4Fe–4S] center overlap. When the magnetic field is set to H_o > 12300 G (g < 2.046), where the EPR signal from the [4Fe–4S] clusters dominates, three ENDOR lines are observed at 13.4, 16.0, and 19.4 MHz (Figure 1E). These signals are assigned to the [4Fe–4S] clusters because they are observed from a sample lacking the Ni–Fe–C signal; they are further assigned to two types of iron sites with $A^{Fe}(1)$ = 30.4 and $A^{Fe}(2)$ = 35.2 MHz as indicated in Figure 1E. At intermediate magnetic fields where the signal from the Ni–Fe–C center and the [4Fe–4S] clusters overlap, we observed a superposition of the ^{57}Fe ENDOR response from both centers. As the field is increased (Figure 1A–E) from g = 2.08 to 2.05, the ^{57}Fe signal of the Ni–Fe–C center at 11.9 MHz diminishes, and that of the [4Fe–4S] cluster at 13.4 MHz increases, confirming that the signals observed at g = 2.08 arise from the Ni–Fe–C center instead of the [4Fe–4S] clusters. The signal at about 19 MHz apparently remains unchanged as the field is increased; most likely, this is because the Ni–Fe–C center and the [4Fe–4S] cluster both have an iron atom with $A^{Fe} \approx$ 35 MHz.

Thus, the combined EPR and ^{57}Fe ENDOR data indicate that the Ni–Fe–C complex contains either three to four Fe that appear as a single type of Fe with $A_\perp^{Fe}$ = 35 and $A_\parallel^{Fe}$ = 27 MHz or two types of Fe with $A^{Fe}(1)$ = 27 and $A^{Fe}(2)$ = 35 MHz. Both interpretations would be consistent with the Mössbauer results (Lindahl et al., 1989a).

^{13}C ENDOR. ENDOR spectra taken at $g_\parallel$ = 2.03 of the Ni–Fe–C signal from CODH treated with ^{13}CO revealed a signal at 27 MHz (Figure 2B). Although the signals from the Ni–Fe–C center and the [4Fe–4S] clusters superimpose with each other at this g value, this ENDOR signal is assigned to ^{13}C associated with the Ni–Fe–C center because it is absent in the sample treated with ^{12}CO and it is not observed from the g < 2.02 region of the EPR signal, where the signals from [4Fe–4S] clusters dominate. This ^{13}C signal is assigned to the ν_+ feature of a doublet, in which case eq 1 gives A^C = 27.5 MHz and ν_- = 0.5 MHz. A peak at 0.5 MHz would have low

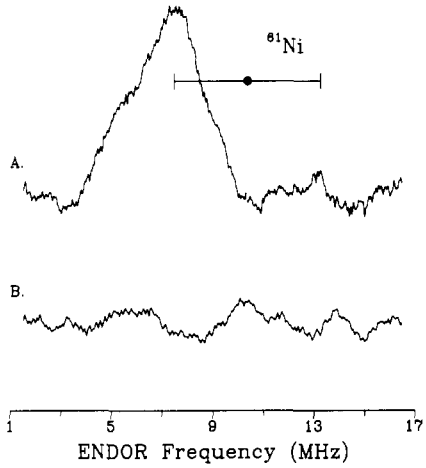

FIGURE 3: ^{61}Ni ENDOR spectrum from ^{61}Ni-enriched CODH (A) and ENDOR spectrum from natural-abundant enzyme (B) at g = 2.07. *Conditions*: microwave frequency, 35.43 (A) and 35.31 GHz (B); H = 12250 (A) and 12210 G (B); rf scan rate, 20 MHz/s; scans, 3000. Other conditions are the same as Figure 1.

intensity and could escape detection. An alternative assignment of the observed signal as the ν_- feature of a doublet leads to A^C = 80.5 MHz, and eq 1 predicts its partner would be at ν^+ = 53.5 MHz, in the center of the intense proton ENDOR pattern where it would be difficult to observe. However, this possibility is ruled out by the close agreement between the experimental and simulated EPR spectra of ^{13}CO–CODH using $A^C_\parallel$ = 27 MHz (Figure 4B) and also a previous simulation which gave $A^C_\parallel \approx$ 25 MHz (Ragsdale et al., 1988).

Because the ^{13}C signal is associated only with the Ni–Fe–C center, it is possible to examine this signal as the field is set across the Ni–Fe–C EPR envelope, 2.08 $\geq g \geq$ 2.03, even though for $g \leq$ 2.04 the EPR intensity arises both from the Ni–Fe–C center, which gives ^{13}C ENDOR, and from the 4Fe clusters, which do not give any ^{13}C ENDOR. The ^{13}C ENDOR signal appears at almost the same frequency at $g_\perp$ of the Ni–Fe–C signal (g = 2.08, Figure 2A), giving $A^C_\parallel \approx A^C_\perp$, except that the line width is about 1 MHz wider; this extra width reflects a very small degree of anisotropy in the ^{13}C hyperfine coupling.

This result confirms the presence of a single bound CO, for the previous EPR simulation of ^{13}CO–CODH gave $A^C_\parallel \approx$ 25 MHz (Ragsdale et al., 1988) on the assumption of one ^{13}C associated with the Ni–Fe–C center. We do not confirm the large anisotropy of A^C, $A^C_\parallel \approx$ 25 and $A^C_\perp$ = 6–13 MHz, that was indicated by the EPR simulation. However, further simulations of the EPR spectrum, using the ENDOR-derived isotropic A value (Figure 4B), show that the ^{13}C EPR broadening in fact can be described with a single ^{13}C having such an isotropic hyperfine coupling.

^{61}Ni ENDOR. Previous EPR studies on ^{61}Ni-enriched *C. thermoaceticum* CODH revealed a hyperfine broadening due to ^{61}Ni. The simulation of the EPR spectrum gives $A_\perp$ = 20 and $A_\parallel$ = 3 MHz, on assumption of a single interacting ^{61}Ni (Ragsdale et al., 1988).

ENDOR resonances from ^{61}Ni are observed by setting the magnetic field to $g_\perp$ of the Ni–Fe–C signal of the ^{61}Ni-enriched CODH sample (g = 2.08), where the EPR signal of the Ni–Fe–C complex has a maximum intensity. The signal centered at ~7.5 MHz (Figure 3A) is weak, but can be assigned to ^{61}Ni because it is absent from the natural-abundance sample under the same experimental conditions (Figure 3B). The partner of the ^{61}Ni resonance is not observed, and thus the observed ^{61}Ni signal could correspond either to the ν_+ or to the ν_- feature.[1] In the former case, the ^{61}Ni hyperfine

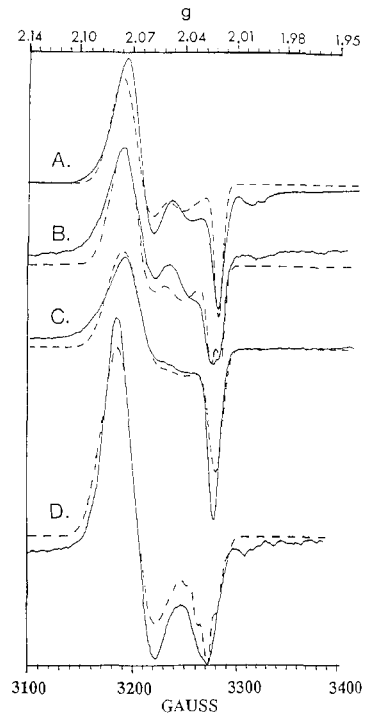

FIGURE 4: X-band EPR spectra of isotopically enriched CODH. The experimental spectra (solid lines) of isotopically enriched CODH are compared with spectral simulations (dashed lines) using A values derived from the ENDOR experiments. (A) *Natural abundance*: 80% of the (2.08, 2075, 2, 028) form (called g 2.08) with line widths of 42, 40, and 12 MHz and 20% of the (2.067, 2.054, 2.028) form (called g 2.067) with line widths of 49, 27, and 13 MHz. (B) *^{13}C enriched.* The simulation included one ^{13}C nucleus (100% isotopic enrichment) with the following parameters: $A_{x,y,z}$ = 27 MHz; 80% of the g 2.08 form; 20% of the g 2.067 form. (C) *^{61}Ni enriched.* The simulation included one ^{61}Ni atom (80% enrichment) with the following parameters: $A_{x,y}$ = 24.3, A_z = 10.5 MHz; 70% of the g 2.08 form; 30% of the g 2.067 form. (D) *^{57}Fe enriched.* The simulation included four ^{57}Fe atoms (90% enrichment) with the following parameters: *site 1*, two Fe $A_{x,y}$ = 34.5, A_z = 29.5 MHz; *site 2*, two Fe $A_{x,y}$ = 28.7, A_z = 25.0 MHz; 100% of g 2.08. EPR conditions: frequency, 9.287 GHz; modulation amplitude, 5 G; power, 10 mW; temperature, 100 K.

coupling constant would be $A^{Ni} \sim$ 5.7 MHz (eq 4), or $A^{Ni} \sim$ 24.3 MHz in the later. The latter assignment, as indicated in Figure 3A, corresponds well to $A_\perp$ as estimated from EPR line broadening and gives fairly good simulations of the X-band EPR spectrum (Figure 4C), whereas the former one would not give sufficient line broadening. One nickel is sufficient to simulate the spectrum, but in this case, two nickels are not ruled out because the simulation with two nickels does not change the spectrum very much.

In principle, one could examine the field dependence of the ^{61}Ni signals from the Ni–Fe–C center for a complete analysis of the A tensor, because the ^{61}Ni ENDOR signal is not detected at high magnetic fields where $g >$ 2.08. Unfortunately, we cannot obtain a good ^{61}Ni ENDOR spectrum anywhere other than at $g_\perp$ of the Ni–Fe–C signal because the EPR signal intensity is much lower at other g values. Thus, in the case of the ^{61}Ni site, ENDOR adds little, beyond an inde-

[1] Because of the details of the spin cross-relaxation, often there is a considerable difference between the intensities of the ν_+ and ν_- branches of the Q-band ENDOR signal. From our experience, the ν_+ feature is normally stronger than the ν_- feature, but not always. For example, the ^{14}N ENDOR signal from tree laccase (Werst & Hoffman, 1990) shows that the relative intensity of ν_+ and ν_- varies across the EPR signal, with the ν_- feature being more intense than the ν_+ feature at $g \sim$ 2.3. Note that the ^{14}N hyperfine tensor is strongly anisotropic, as is that inferred from line broadening, and these intensity variations are known to occur in such a case.

pendent corroboration, to the EPR results.

The ENDOR signals from ^{61}Ni strongly depend on the rate with which the radio-frequency field is swept and are seen most easily with a rapid scan (≈20 MHz/s) that presumably cause rapid passage effects in the nuclear spin system. It is interesting that the ENDOR signals from ^{63,65}Cu, which also have $I = {}^3/_2$, exhibit a similar dependence on sweep rate (Hoffman et al., 1980), which suggest common nuclear relaxation properties for such nuclei.

^{1}H ENDOR. The proton ENDOR pattern (data not shown) obtained from the Ni–Fe–C signal is poorly resolved and is not distinctive; the width of the proton pattern corresponds through eq 1 to proton resonances with hyperfine coupling of $A^H < 6$ MHz.

Conclusions

We have provided unambiguous evidence that when CODH reacts with CO, a novel metal center is formed which includes at least one nickel, at least three iron sites, and the carbon of one CO. The A^{Fe} values determined by ENDOR are similar to the values used in simulation of the Mössbauer spectra (Lindahl et al., 1989a), and based on Mössbauer analysis of this center, the iron components were postulated to be in the form of a $[4Fe–4S]^{2+}$ structure. EPR simulations using these A^{Fe} values are equally good for a 4Fe or a 3Fe center. A 3Fe–xS center is ruled out by the Mössbauer data (Lindahl et al., 1989a) unless there is another metal (e.g., Ni) incorporated into the fourth site of the cube.

The ^{13}C ENDOR data are consistent with a single CO bound to either the Ni or the Fe components of the spin-coupled cluster. We do not yet know the form of CO that is ligated to the metals in the complex. However, the A^C values are similar to those determined earlier for the CO-bound form of the H cluster of the *Clostridium pasteurianum* hydrogenase, proposed to be the active site of hydrogen activation (Telser et al., 1987).

The ^{61}Ni ENDOR data are the first nickel ENDOR recorded for an enzyme. Only a single ENDOR line is observed, and the EPR simulations using the ENDOR-derived A^{Ni} values are consistent with a single nickel site in the Ni–Fe–C complex.

On the basis of our results and the Möessbauer data (Lindahl et al., 1989a), we proposed the stoichiometry of the components of the Ni–Fe–C complex to be $Ni_1Fe_{3-4}S_{\geq 4}C_1$, with four acid-labile sulfides as part of the Ni–Fe–C center. For example, our results would be consistent with but are not restricted to a structure such as $NiFe_3S_4$ in which the Ni is incorporated directly into a cubane structure or a structure in which the Ni is bridged to a [4Fe–4S] center by a ligand. A pertinent recent result is the incorporation of Ni into the [3Fe–4S] center of the *Pyrococcus furiosus* ferredoxin, forming a $[NiFe_3S_4]$ cluster (Conover et al., 1990).

Acknowledgments

We thank Mr. Clark Davoust, whose expertise was essential to the construction and operation of the Q-band ENDOR apparatus.

Registry No. CODH, 64972-88-9; CO, 630-08-0.

References

Altman, T. E. (1981) Ph.D. Thesis, University of Illinois, Urbana.

Bastian N. R., Diekert, G., Niederhoffer, E. G., Teo, B.-K., Walsh, C. P., & Orme-Johnson, W. H. (1988) *J. Am. Chem. Soc. 110*, 5581–5582.

Belford, R. L., & Nilges, M. J. (1979) *Computer simulation of powder spectra*, EPR Symposium, 21st Rocky Mountain Conference, Denver, CO.

Conover, R. C., Park, J.-B., Adams, M. W. W., & Johnson, M. K. (1990) *J. Am. Chem. Soc.* (in press).

Cramer, S. P., Eidsness, M. K., Pan, W.-H., Morton, T. A., Ragsdale, S. W., DerVartanian, D. V., Ljungdahl, L. G., & Scott, R. A. (1987) *Inorg. Chem. 26*, 2477–2479.

Duliba, E. P. (1981) Ph.D. Thesis, University of Illinois, Urbana.

Feher, G. (1959) *Phys. Rev. 114*, 1219–1244.

Hoffman, B. M., Roberts, J. E., Swanson, M., Speck, S. H., & Margoliash, E. (1980) *Proc. Natl. Acad. Sci U.S.A. 77*, 1452–1456.

Hoffman, B. M., Gurbiel, R. J., Werst, M. M., & Sivaraja, M. (1990) *Advanced EPR* (Hoff, A. J., Ed) Elsevier, Amsterdam.

Lindahl, P. A., Ragsdale, S. W., & Munck, E. (1989a) *J. Biol. Chem. 265*, 3880–3888.

Lindahl, P. A., Munck, E., & Ragsdale, S. W. (1989b) *J. Biol. Chem. 265*, 3873–3879.

Ljungdahl, L. G., & Andreesen, J. R. (1978) *Methods Enzymol. 53*, 360–372.

Lu, W. P., & Ragsdale, S. W. (1990) *J. Biol. Chem.* (in press).

Maurice, A. M. (1981) Ph.D. Thesis, University of Illinois, Urbana.

Nilges, M. J. (1981) Ph.D. Thesis, University of Illinois, Urbana.

Ragsdale, S. W., & Wood, H. G. (1985) *J. Biol. Chem. 260* (*7*), 3970–3977.

Ragsdale, S. W., Ljungdahl, L. G., & DerVartanian, D. V. (1982) *Biochem. Biophys. Res. Commun. 108* (*2*), 658–663.

Ragsdale, S. W., Clark, J. E., Ljungdahl, L. G., Lundie, L. L., & Drake, H. L. (1983a) *J. Biol. Chem. 258* (*4*), 2364–2369.

Ragsdale, S. W., Ljungdahl, L. G., & DerVArtanian, D. V. (1983b) *Biochem. Biophys. Res. Commun. 115* (*5*), 658–665.

Ragsdale, S. W., Wood, H. G., & Antholine, W. E. (1985) *Proc. Natl. Acad. Sci U.S.A. 82* (*10*), 6811–6814.

Ragsdale, S. W., Wood, H. G., Morton, T. A., Ljungdahl, L. G., & DerVartanian, D. V. (1988) in *The Bioinorganic Chemistry of Nickel*, pp 311–332, VCH Publishers, New York.

Shanmugasundaram, T., Ragsdale, S. W., & Wood, H. G. (1988) *Biofactors 1*, 147–152.

Stephens, P. J., McKenna, M. C., Ensign, S. A., Bonam, D., & Ludden, P. W. (1987) *J. Biol. Chem. 264*, 16347–16350.

Telser, J., Benecky, M. J., Adams, M. W. W., Mortenson, L. E., & Hoffman, B. M. (1987) *J. Biol. Chem. 263*, 6589–6594.

Terlesky, K. C., Barber, M. J., Aceti, D. J., & Ferry, J. G. (1987) *J. Biol. Chem. 262*, 15392–15395.

Venters, R. A., Nelson, M. J., McLean, P., True, A. E., Levy, M., Hoffman, B. M., & Orme-Johnson, W. H. (1986) *J. Am. Chem. Soc. 108*, 3487–3498.

Werst, M., & Hoffman, B. M. (1990) *J. Am. Chem. Soc.* (in press).